Bat algorithm based maximum power point tracking for photovoltaic system under partial shading conditions

Kaced, Karim ; Larbes, Cherif; Ramzan, Naeem; Bounabi, Moussaab; Dahmane, Zine elabadine

Published in:
Solar Energy

DOI:
10.1016/j.solener.2017.09.063

Published: 01/12/2017

Document Version
Peer reviewed version

Bat algorithm based maximum power point tracking for photovoltaic system under partial shading conditions

Karim KACED[a,*], Cherif LARBES[a], Naeem RAMZAN[b], Moussaab BOUNABI[a], Zine elabadine DAHMANE[a]

[a]*Ecole Nationale Polytechnique, Electronic department, 10, avenue Pasteur, Hassan Badi, 16200 Algiers, Algeria.*
[b]*School of Engineering and Computing, University of the West of Scotland, Paisley, PA1 2BE, UK.*

Abstract

This paper presents a maximum power point tracking (MPPT) method for photovoltaic system under partial shading conditions using bat algorithm (BA). The bat algorithm is a swarm intelligence based method which was inspired by the echolocation behaviour of bats. BA have a high accuracy in the global optimisation and it can provide good dynamic performance and very quick convergence rate by automatically switching between exploration and exploitation stages during the MPPT process. To verify the performance of the proposed method, several simulations have been carried out in Matlab/Simulink environment for various shading patterns. The simulations results highlight the accuracy of the proposed scheme for optimal management of the energy available at the output of the photovoltaic panels. In addition, the comparison with the P&O and the PSO methods shows that the proposed method outperforms them in term of global search ability and

*Corresponding author. Tel: +213 551791351
Email address: karim.kaced@g.enp.edu.dz (Karim KACED)

dynamic performance. To verify the practical implementation of the proposed method, a modular reconfigurable architecture is designed using very high speed description language (VHDL) and implemented on Xilinx Virtex-5 (XC5VLX50-1FFG676) Field Programmable Gate Array (FPGA). The use of FPGA for designing the MPPT controller provides high performance, increases the robustness and makes the hardware implementation more felxible. The algorithm is tested in real time application on a buck-boost converter using a real photovoltaic panel. Experimental results confirm the efficiency of the proposed method in the global peak tracking and its high accuracy to handle the partial shading.

Keywords:

Partial shading conditions, bat algorithm (BA), maximum power point tracking (MPPT), photovoltaic (PV) system, field programmable gate array (FPGA).

---

1. Introduction

RENEWABLE energy resources have enormous potential and offer many advantages over conventional energy resources. Renewable energy comes from several resources like solar, wind, geothermal, biomass and water. They can produce electricity in large quantities over a long term without too emit greenhouse gases. The renewable sources of energy derived from the sun can be used both directly and indirectly. The direct use of solar energy by means of sensors is related to two distinct technologies: the first produces calories, it's solar thermal energy, and the second produces electricity through the photovoltaic effect. Photovoltaic (PV) technology is one of the most promising renewable energy technologies. Photovoltaic systems are configured as stand-alone, grid-connected and hybrid systems [1].

Various configurations are used for the PV modules interconnection to meet the voltage-current requirement [2]. The overall characteristics of photovoltaic generators are varying and depend on several factors, especially the metrological conditions such as solar radiation, ambient temperature and wind speed, the aging of photovoltaic cells and partial shading or inhomogeneity of the illumination. When PV modules receive a uniform sunlight, the resulting P-V characteristic is uni-modal and characterized by a single point of maximum power. When part or the entire module receives a non-uniform illumination, some cells (dimly lit) become reversed bias and turn into receiving elements. This phenomenon is called "hot spot" and can result in the destruction of these cells. To remedy this problem, the photovoltaic modules are equipped with bypass diodes which function is to protect the cells that become passive [3]. The integration of bypass diodes in solar mod-

ule has as consequence the changing of the P-V characteristic which becomes multimodal when the partial shading occurs [4]. The P-V characteristic is then characterized by the appearance of several maxima: several local maximum power points (LMPPs) and one global maximum power point (GMPP). The number of maxima depends on the type of shading (uniform or partial), distribution of the illumination on the photovoltaic generator and the number of bypass diodes incorporated in each photovoltaic module.

Despite efforts to improve the technology of photovoltaic cells, the electrical efficiency is still low [5]. Also, partial shading has dramatic consequences on the electrical power delivered [6, 7]. To reduce losses caused by partial shading and increase the efficiency of photovoltaic panels, several approaches are presented in the literature. These approaches include system architectures, converter topologies, PV array configurations and maximum power point tracking (MPPT) techniques [8]. Despite the improvements that can be achieved by the first three approaches, additional material increases the complexity of the system which becomes more expensive. So a good compromise cost-efficiency can be achieved by development of MPPT techniques which can handle the partial shading.

Several MPPT techniques are presented in the literature to handle the multimodal P-V characteristic in partial shading conditions. These methods vary in complexity, in the types and the number of sensors used and the equipment used for the implementation. [9] proposed a two stage MPPT algorithm for tracking the GMPP. The authors introduce an analytic condition to distinguish partially shaded conditions from normal conditions. This condition is based on the comparison of the sensed photovoltaic current around

$(0.8 \times N_{SS} \times V_{oc})$ and a reference value calculated at uniform insolation conditions with $G = 1000$ W/m^2, where N_{SS} is the number of series photovoltaic module and V_{oc} is the open circuit voltage. When the region of GMPP is located, the algorithm calls a hill climbing subroutine to reach the GMPP. However, in the first stage, $(N_{SS} + 1)$ points should be tested each time the partial shading conditions are detected before calling the hill climbing algorithm to locate the GMPP. This method will become time-costly if the number of series module is large [10]. In addition, temperature sensors must be used to determine the open circuit voltage. Another two-stage search method is proposed by [11] for locating the GMPP. The first stage involved using a fixed spacing method to divide the P–V characteristic curve into various segments and to obtain the block in which GMPP is located. During the second stage, a variable step-size perturb and observe (P&O) method is used to locate the precise location of the GMPP. The authors recommended using $(N_{SS} + 1)$ segments at the first stage to enhance the tracking performance, where N_{SS} denotes the number of PV modules serially connected. It is shown in [12] that the function describing the PV power as a function of the PV voltage is a Lipschitz function. Therefore, [12] adopted the dividing rectangles (DIRECT) algorithm to search for the GMPP. Although the presented experimental results showed the efficiency of this method in tracking the GMPP under partial shading conditions, an appropriate choice of the first sampling interval is primordial for the GMPP tracking performance [13]. [14, 15, 16] employed two-stage search methods to track the GMPP, which first scanned the P–V characteristic curve and then recorded the GMPP. In the second stage, these methods applied either the P&O method [14] or

fuzzy logic control [15, 16] to maintain the operating point at the GMPP. Evolutionary algorithms (EA) have attracted special attention by the academic community in recent years. Indeed, several articles have appeared in scientific journals, highlighting the effectiveness of these algorithms in the tracking of maximum power point in partially shaded conditions. Thanks to its simple structure, the particle swarm optimisation (PSO) algorithm is developed and improved by many researchers. [17] used conventional PSO algorithm to control several PV arrays with one pair of voltage and current sensors. In [18], the authors used the PSO technique for the tracking of GMPP using direct duty cycle control method. PI control loops are eliminated and the duty cycle of the Pulse Wide Modulation (PWM) signal is adjusted directly by the MPPT algorithm. In [19], the authors have improved their algorithm (PSO) by removing random factors from the velocity equation. The proposed algorithm becomes deterministic and its structure becomes simpler. However, a restriction is imposed on the maximum of particle velocity to not fall into a LMPP. [13] combined P&O and PSO to form a hybrid method to reduce the search space of the PSO. Initially, the P&O method is employed to identify the nearest local maximum. Then, the PSO method is used to search for the GMPP. Experimental results show that this method has a faster convergence time and better dynamic response than the conventional PSO algorithm. Adaptive approaches are reported in [20, 21] to tune the PSO algorithm control parameters to increase the efficiency and performance of the GMPP tracking. In [20] , the authors proposed to adjust these parameters in linear way whereas the authors in [21] suggested varying them in exponential form. Despite improvements provided by these

approaches, the structure of the algorithm becomes more complex and parameter selection task becomes more difficult [10]. [22, 23, 24] tracked the GMPP using differential evolution (DE) algorithm. The conventional DE is used in [22] whereas modified mutation strategy are adopted in [23, 24] to improve the convergence speed. [24] proposed to remove the random numbers from the algorithm, and then the donor vectors (generated by the mutation) are used directly as a trial vectors. Experimental results of ten shaded patterns show that this method outperforms the PSO method in terms of global tracking capability and convergence time. [25] proposed a maximum power point tracking (MPPT) for PV system using cuckoo search method (CS). CS is a population based algorithm and its concept is similar to PSO. The main difference between CS and PSO is the manner to update the step sizes. In fact, the step sizes in CS are performed by Lévy Flight. The results shows improvements compared to the PSO technique in terms of convergence speed and transient fluctuations, but the structure of the CS algorithm is more complex. [26] presented a MPPT algorithm based on a colony of flashing fireflies for tracking GMPP in partially shaded PV arrays, and compared it with PSO algorithm. The published results indicates that the firefly algorithm based tracking outperforms the PSO method in terms of tracking speed and dynamic behaviour. [27] proposed a hybrid method called DEPSO, a combination of PSO and DE. The PSO algorithm is used in odd iterations and the DE algorithm is performed in even iterations. Although this algorithm can track the GMPP, the presented results show that DEPSO requires a lot of iterations to converge, producing large fluctuations in the power before reaching the steady state [28].

The main drawback of the mentioned EA based MPPT is that the trade-off exploration-exploitation is low, which may result in large fluctuations in the operating power of the PV array during the optimization process, or to fall in LMPP in some partial shading configurations. [29] has developed a new metaheuristic method, the Bat Algorithm (BA), which is inspired on the echolocation behaviour of microbats. BA uses a frequency-tuning technique to increase the diversity of the solutions in the population. As a result, the search space is excellently explored. Moreover, this algorithm provides a mechanism of automatic switching between explorative moves and exploitation during the MPPT process. This feature allows to the algorithm to have a quick convergence rate towards the GMPP without falling into the trap of premature convergence. In addition, the combination of exploration (global search) and exploitation (local search) during the tracking process also allows to the algorithm to present good dynamic behaviour and less oscillations before reaching the GMPP.

Recognizing these benefits, this paper proposes bat algorithm based MPPT to track GMPP under partial shading conditions. The remainder of this paper is structured as follows. Section II presents the modelling of the photovoltaic system and the behaviour of the photovoltaic panel under partial shading condition. Section III discusses the key features of the bat algorithm and describes the proposed bat algorithm for MPPT. Section IV highlights the effectiveness of the proposed algorithm in the global peak tracking and its superiority over the PSO and P&O algorithms. Experimental validation is presented in section V and finally, a conclusion is made in section VI.

2. Modelling of the photovoltaic system

2.1. PV module model

The general equivalent electrical circuit of the two-diode model, shown in Fig. 1 is used to simulate the behaviour of the solar cell. This model contains a current source I_{PV}, which describes the photocurrent, two diodes D1 and D2, a series resistance R_S and a parallel resistance R_P. An accurate model of PV array based on this model is presented in [30]. Eq. (1) describes the output current of the PV array:

$$I = I_{PV}N_{PP} - I_{o1}N_{PP}\left[exp\left(\frac{V + IR_SN_S\left(\frac{N_{SS}}{N_{PP}}\right)}{a_1V_TN_SN_{SS}}\right) - 1\right]$$

$$-I_{o2}N_{PP}\left[exp\left(\frac{V + IR_SN_S\left(\frac{N_{SS}}{N_{PP}}\right)}{a_2V_TN_SN_{SS}}\right) - 1\right] - \left(\frac{V + IR_SN_S\left(\frac{N_{SS}}{N_{PP}}\right)}{R_PN_S\left(\frac{N_{SS}}{N_{PP}}\right)}\right) \quad (1)$$

where I and V refer to the output current and the output voltage of the PV array, respectively. N_S is the number of solar cells connected in series incorporated in each PV module, whereas N_{SS} and N_{PP} denote the number of PV modules connected in series and parallel, respectively. V_T (equal to KT/q) is the thermal voltage of the diodes, k is the Boltzmann constant ($1.3806503 \times 10^{-19}$ J/K), q is the electron charge ($1.60217646 \times 10^{-19}$ C) and T is the temperature in Kelvin. a_1 and a_2 are the ideality factors of the diodes D1 and D2, respectively.

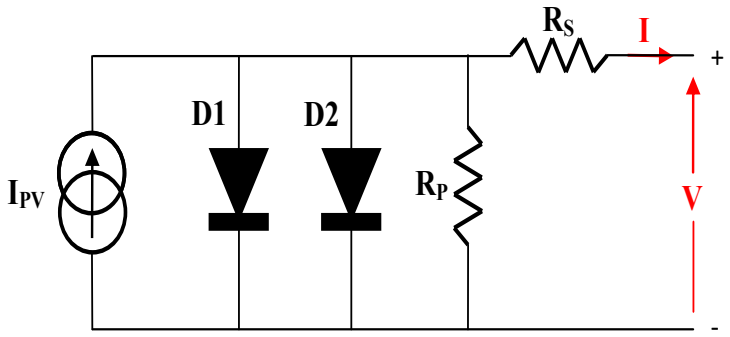

Figure 1: Equivalent circuit of a solar cell.

The photocurrent I_{PV} is directly influenced by the solar irradiance G and the temperature T. It is given by

$$I_{PV} = I_{sc\_STC} + K_1 \left(T - T_{STC}\right). \tag{2}$$

The diodes saturation currents I_{01} and I_{02} are given by

$$I_{o1} = I_{o2} = \frac{I_{sc\_STC} + K_I \left(T - T_{STC}\right)}{exp\left(\frac{V_{oc\_STC} + K_V (T - T_{STC})}{N_S V_T}\right)} \tag{3}$$

where $I_{sc_STC}$and V_{oc_STC} are the short circuit current and the open circuit voltage of the PV module in the standard test condition (STC), i.e. $T = T_{STC} = 298.15$ °K and $G = G_{STC} = 1000$ W/m^2.

The PV module used in this paper is SM55. The parameters of this module under STC are given in Table 1. Fig. 2 shows the corresponding static P-V curves for different values of irradiance G and temperature T. The module receives a uniform solar insulation, thus, the P-V curves exhibit an unique maximum power point (MPP).

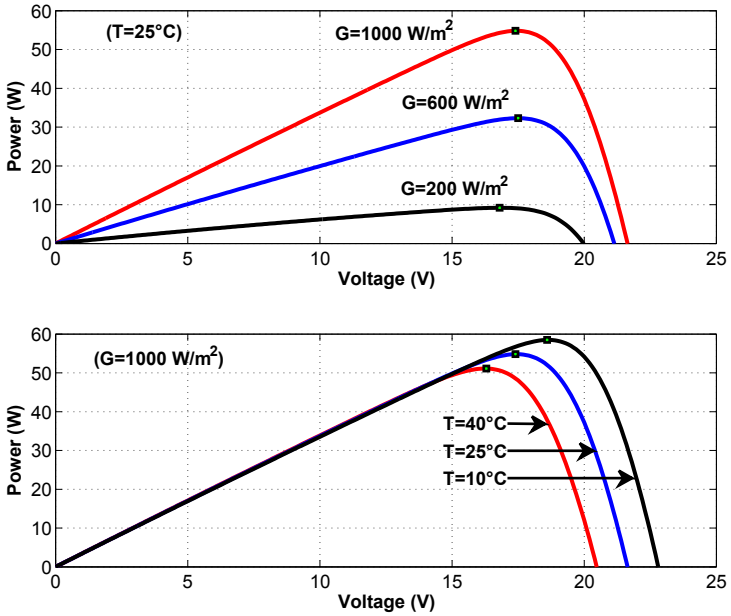

Figure 2: The P-V characteristics under uniform condition.

To protect photovoltaic modules against "hot spot" phenomenon, they are equipped with bypass diodes. The photovoltaic module used is consisting of 36 cells connected in series, and protected by two bypass diodes. Each diode is connected in antiparallel with a group of 18 solar cells. The presence of these protection diodes changes the shape of the P-V characteristic and makes it more complicated when PV panel is subjected to partial shading. In partially shaded conditions, the resulting P-V characteristic presents several points of maximum power, several local maxima and one global maximum. Fig. 3(a) shows a photovoltaic panel consisting of two serially connected modules SM55. The resulting panel can be considered as four (4) sub-modules and each sub-module is protected by one bypass diode.

In a first case, we assume that the first module receives a uniform ir-

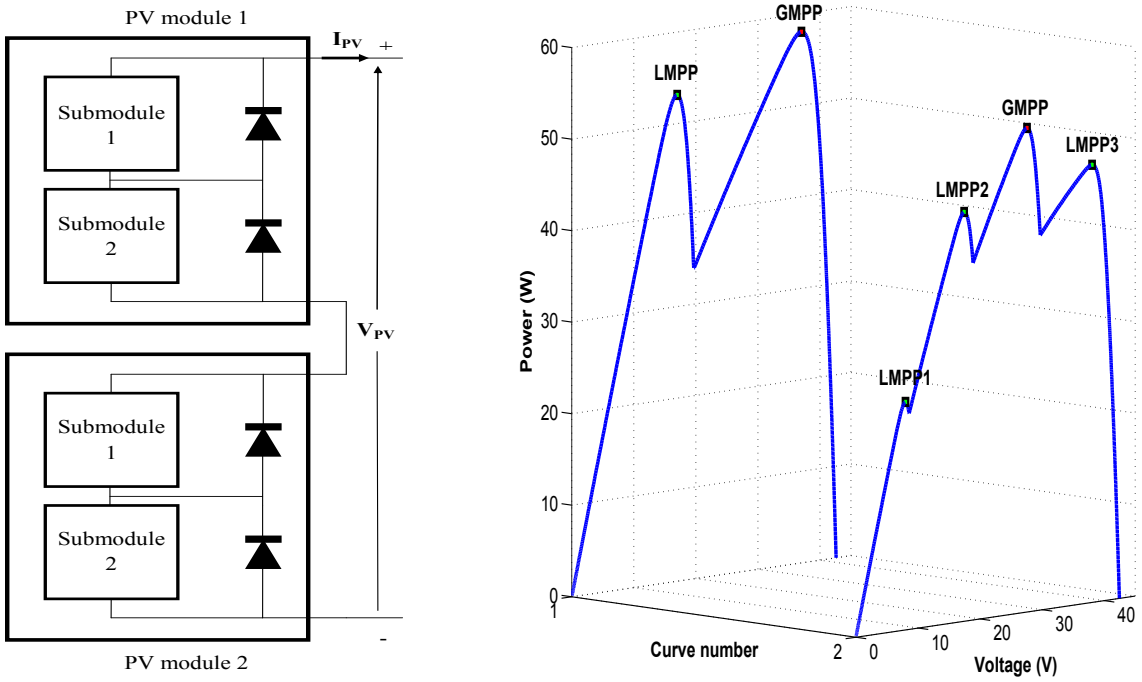

(a) (b)

Figure 3: (a) Model of PV panel consisting of two photovoltaic modules connected in series and (b)P-V curves of PV panel under two partial shading patterns.

radiance of $G_1 = 1000$ W/m^2 while the second receives an insulation of $G_2 = 500$ W/m^2 . The resulting P-V characteristic is shown in Fig. 3(b). We can notice the appearance of two maximum power point $P_1 = 53.14$ W and $P_2 = 58.04$ W at $V_1 = 17$ V and $V_2 = 37$ V, respectively. Fig. 3(b) shows the P-V curve in the case where each sub-module receives a different irradiance, for example $G_{11} = 1000$ W/m^2 , $G_{12} = 800$ W/m^2 , $G_{21} = 600$ W/m^2 et $G_{22} = 400$ W/m^2 (the notation G_{ij} refers to the insulation G for the sub-module j of the module i). In this case, the P-V characteristic is

Table 1: SM55 module specifications.

Parameters	Value
Maximum power (P_{mpp})	55 W
Short circuit current (I_{sc})	3.45 A
Open circuit voltage(V_{oc})	21.7 V
Maximum power current (I_{mpp})	3.15 A
Maximum power voltage (V_{mpp})	17.4 V
Temperature coefficient of I_{sc} (K_I)	1.2×10^{-3} A/°C
Temperature coefficient of V_{oc} (K_V)	-77×10^{-3} V/°C
Number of series cells in the module (N_s)	36
Number of bypass diodes	2

characterized by the appearance of four maximum power point whose the global is $P = 52.89$ W at $V = 27.59$ V. Thus, the P-V characteristic can take various forms according to the shading pattern and the tracking of the global maximum power point (GMPP) becomes a more challenging task.

2.2. DC-DC converter modelling

Fig. 4 shows a simplified electric schematic of a basic inverting buck-boost converter. In addition to input and output capacitors, the power stage consists of a power metal-oxide semiconductor field-effect transistor (MOSFET), a diode, and an inductor.

The buck-boost converter assumes two states per switching cycle. The ON State is when Q is close and the OFF State is when Q is open. The duration of the ON state is d T_s, where d is the duty cycle of PWM signal

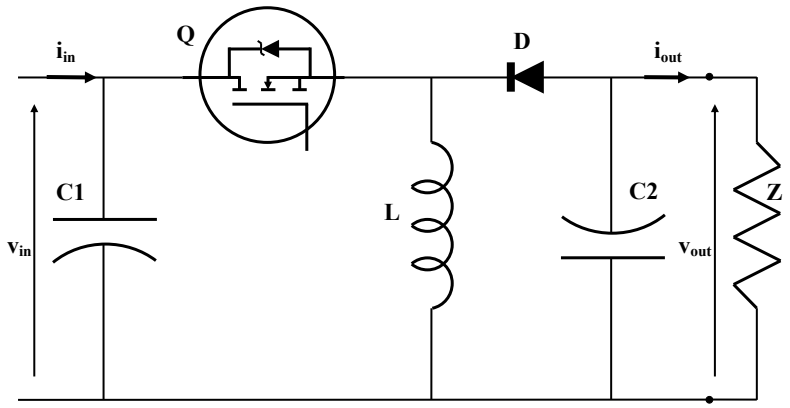

Figure 4: Electrical circuit of a Buck-Boost converter.

and T_s is the switching period.

During the closing time $d \times T_s$ of the transistor, the source voltage V_{in} is applied across the inductor L, which results in accumulating energy in the inductor. During the opening period $(1-d)T_s$, the diode D is forward-biased and the voltage of the inductance is applied to the load Z. The current flows anticlockwise through the diode D. Thus, the output voltage will be negative.

The dynamics of the converter in one switching period is represented by the following system :

$$\begin{cases} C_1 \frac{dv_{in}(t)}{dt} = i_{in}(t) - d \times i_L(t) \\ C_2 \frac{dv_{out}(t)}{dt} = -(1-d)\, i_L(t) - i_{out}(t) \\ L \frac{dv_L(t)}{dt} = d \times v_{in}(t) + (1-d)\, v_{out}(t) - R_L i_L(t) \end{cases} \tag{4}$$

where $i_{in}(t)$, $i_{out}(t)$ and $i_L(t)$ are the input, the output and the inductor current, respectively. $v_{in}(t)$, $v_{out}(t)$ and $v_L(t)$ are the input, the output and the inductor voltgae, respectively.

3. The proposed bat algorithm based MPPT

3.1. Overview of Bat search algorithm

Bat algorithm is a population based optimization algorithm inspired by the echolocation features of microbats in locating their foods. It is developed by Yang in 2010 [29].

Small bats (microbats) feed primarily on insects which detect using echolocation. The direction and intensity of the return signal enable them to locate potential prey in direction, and also in distance. At first, the bat overflies the search space, while emitting a set of ultrasonic pulses of a certain amplitude (intensity) and a rate (density). Between the pulse trains, it receives the feedback signals (its own signal and eventually the signals from other bats in the swarm) by echolocation and interprets them. If the signals received in return have a low intensity and a strong rate, then it is very likely that prey is detected and the bat should head toward it. As the bat approaches the prey, it gradually intensifies the amount of pulses (the ultrasound rate) and, at the same time, progressively decreases the intensity of these pulses.

Bat algorithm is developed then by idealizing some of the echolocation characteristics of microbats [29]. Bat algorithm maintains a swarm of N microbats, where each microbats flies randomly with a velocity v_i at position x_i, with a varying loudness A_i and pulse emission rate $r_i \in [0, 1]$ depending on the proximity of their target.

During the optimization task, every bat is randomly assigned a frequency which is drawn uniformly from $[f_{min}, f_{max}]$. Then, the velocity v_i and the position x_i of each bat at time step t are defined and updated with

$$f_i = f_{min} + (f_{max} - f_{min})\,\beta \tag{5}$$

$$v_i^{t+1} = v_i^t + \left(x_i^t - x_*\right) f_i \tag{6}$$

$$x_i^{t+1} = x_i^t + v_i^{t+1} \tag{7}$$

where $\beta \in [0, 1]$ is a vector randomly drawn from a uniform distribution. x_* is the current global best location (solution) which is achieved after comparing all the solutions among all the N bats at each iteration t.

If a random number is greater than the pulse emission r_i^t, then the exploitation stage is selected and the position x_i^{t+1} is replaced by the solution generated by the local search. As a result, a new solution is drawn locally by using a random walk around the current best solution [31]

$$x_{new} = x_* + \epsilon A^t \tag{8}$$

where ϵ is a random number which can be drawn from a uniform distribution in $[-1, 1]$ or a Gaussian distribution, while $A^t =< A_i^t >$ is the average loudness of all the bats at this time step [32].

If a random number is smaller than the loudness A_i^t and the new solution improve the fitness value, this means that the bat is moving towards the prey (the optimal solution). Then, the new solution is accepted and its loudness and emission rates are updated to control the exploration and exploitation. It is suggested that loudness decreases from positive value A_i^0 to $A_{min} = 0$ whereas the pulse rate of pulse emission increases from 0 to R_i

$$A_i^{t+1} = \alpha A_i^t \tag{9}$$

$$r_i^{t+1} = R_i \left[1 - exp\left(-\gamma t\right)\right] \tag{10}$$

where α is a constant in the range of $[0, 1]$ and γ is a positive constant. In this work, A_i^0 and R_i are set to 1.

3.2. Application for MPPT

The bat algorithm is applied to the tracking of GMPP by the direct duty cycle control method. Thus, the optimization variable is defined as the duty cycle of the PWM signal. The complete flowchart of the proposed bat algorithm based MPPT is illustrated in Fig. 5.

Initialisation

Initially, a vector of N duty cycles (first vector of solutions) is generated from a uniform distribution on $[0, 1]$ or it is predefined. The number of bats (N) is an important factor in the optimization process. A large number N guarantee the determination of GMPP but the convergence time can be long while a small number N will save in convergence time but it can result in low GMPP tracking accuracy if the parameters of the MPPT algorithm are not well optimised. To ensure a compromise "convergence speed-efficiency", the number of duty cycle, N is chosen to be three (3).

For the choice of first vector of duty cycles (first vector of solutions), the method of the reflective impedance is used [12]. The first three duty cycles are calculated thus:

$$d_1 = \frac{\sqrt{\eta Z_{min}}}{\sqrt{R_{PV\_max}} + \sqrt{\eta Z_{min}}} \tag{11}$$

$$d_2 = \frac{\sqrt{\eta Z_{ave}}}{\sqrt{R_{PV\_STC}} + \sqrt{\eta Z_{ave}}} \tag{12}$$

$$d_3 = \frac{\sqrt{\eta Z_{max}}}{\sqrt{R_{PV\_min}} + \sqrt{\eta Z_{max}}} \tag{13}$$

where η is the converter efficiency, Z_{min}, Z_{max} and $Z_{ave} = (Z_{min} + Z_{max})/2$ are the minimum, maximum and averege values of the connected load respectively. R_{PV_min} and R_{PV_max} are the minimum and maximum values of the reflective impedances of the PV array, respectively, while R_{PV_STC} is the reflective impedances of the PV panel at STC condition. In our simulations, the values of the parameters are : $\eta = 0.96$, $Z_{min} = 40\ \Omega$, $Z_{max} = 70\ \Omega$, $R_{PV\_min} = 6\ \Omega$, $R_{PV\_STC} = 22\ \Omega$ and $R_{PV\_max} = 43\ \Omega$.

It should be mentioned that the interval $[d_1, d_3]$ serves only for a first approximation of the search space. This approach leads to prevent having major disturbances and fluctuations in the voltage of the photovoltaic panel. The BA based MPPT can then search for the MPP outside of this range. The minimum duty cycle and maximum duty cycle are defined as 0.02 and 0.98, respectively.

The current and voltage of the photovoltaic array are sensed and the corresponding power is calculated for each duty cycle. The best duty cycle, d_{best} which gives the best value of fitness (PV power) is then stored.

Generating of new solutions

A new vector of solutions is globally generated following the equations

$$f_i = f_{min} + (f_{max} - f_{min})\,\beta \tag{14}$$

$$v_i^k = \omega v_i^{k-1} + \left(d_{best} - d_i^{k-1}\right) f_i \tag{15}$$

$$d_{inew}^k = d_i^{k-1} + v_i^k. \tag{16}$$

Modifications are made on the equation of velocity v_i (Eq. (14)) to take into account the practical limits. The parameter ω called "inertia weight

factor" [33] is used to limit the speeds of microbats while the term ($d_{best} - d_i^{k-1}$) serves as a search direction and ensures that solutions still move towards the best duty cycle d_{best}.

To ensure an automatic and dynamic failover between the exploration stage and the exploitation stage, a local solution is generated locally for each bat when the rate of its emission pulse r_i is lower than the rate of reception pulse randomly generated from a uniform distribution. This local solution is generated by "Random Walk" around the best solution (d_{best}) according to the relationship Eq. (17), and replaces that of the global search.

$$d_{inew}^k = d_{best} + \epsilon \Phi A^{k-1} \tag{17}$$

where $\epsilon \in [-1, 1]$ is a uniform random number, $A^{k-1} =< A_i^{k-1} >$ is the average loudness of all the bats at this step while Φ is a fixed positive constant used to limit the random walk. This constant is set to be 0.05.

Updating of solutions

The new duty cycles are accepted or rejected not only according to the obtained values of PV power, but also depending on the amplitude of the received ultrasonic signals. This amplitude (received) is generated randomly for each duty cycle and compared with the value of the transmitted signal (A_i). Thus, for each new duty cycle, if it improves the objective function ($P(d_{inew}^k) > P(d_i^{k-1})$) and the amplitude of its received signal is less than a random number, then it is accepted and will be a new solution for the next generation. The rate of pulsation of emission of this duty ratio is increased while the amplitude of the ultrasound signal is decreased according to the relationships Eq. (9), Eq. (10).

Convergence criterion

The algorithm continues to calculate the new duty cycles until constraint on convergence is satisfied. In this article, the condition shown in the Eq. (18) is used as a convergence criterion. If the absolute difference between each two different duty cycles is less than a threshold Δd, then the algorithm stops the optimization process and brings out d_{best}

$$\left|d_i^k - d_j^k\right| \leq \Delta d \qquad ; \quad i, j = 1, 2, 3 \quad (i \neq j). \tag{18}$$

Re-initialization

Due to varying weather and loading conditions, the global MPP is usually changing. The MPPT algorithm should have the ability to detect the variation of shading pattern and to search for the new global MPP. In this paper, the search process is initialised if the following condition is satisfied

$$\frac{|P_{PVnew} - P_{PVlast}|}{P_{PVlast}} > \Delta P \tag{19}$$

where P_{PVnew} and P_{PVlast} are the values of photovoltaic panel power in two successive sample periods and ΔP is the power tolerance.

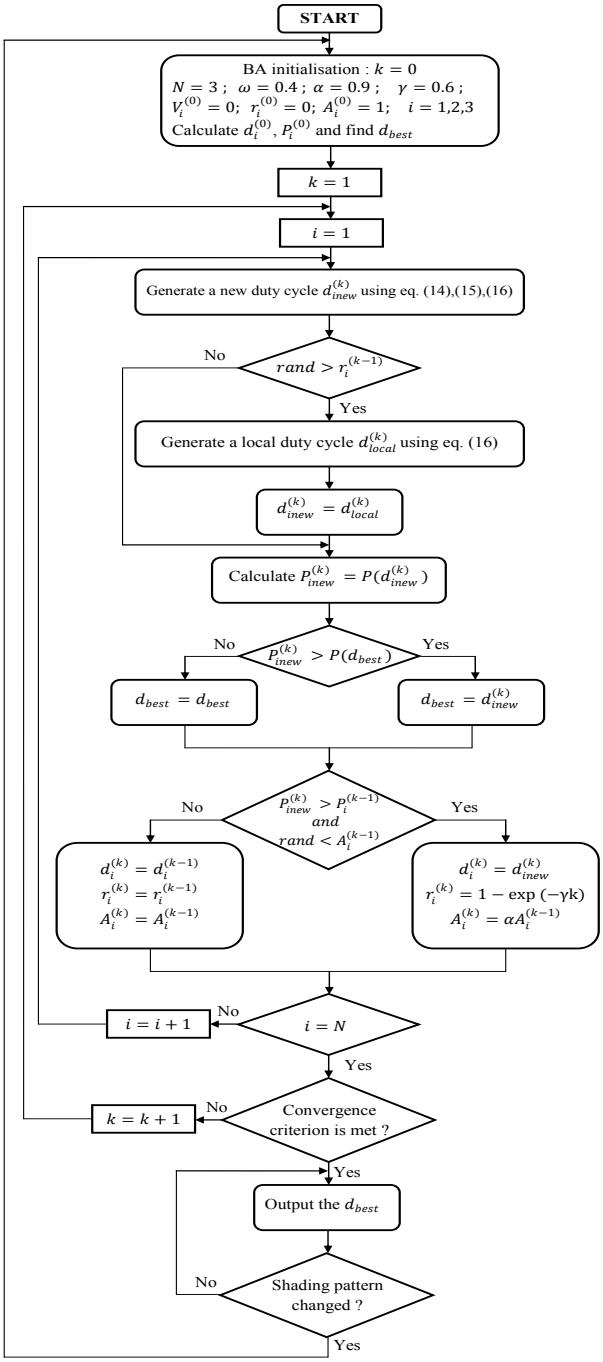

Figure 5: Complete flowchart of the proposed method.

4. Simulation results

To verify the effectiveness of the proposed algorithm, a photovoltaic system is simulated on Matlab/Simulink. The different blocks constituting the model are shown in Fig.6. The photovoltaic panel used consists of four SM55 photovoltaic modules connected in series. The photovoltaic module is modeled according to the model of two diode (section II) and the photovoltaic panel output voltage is determined by the Newton-Raphson iterative method [30, 34].

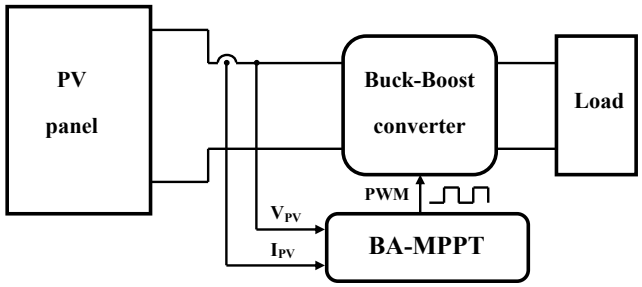

Figure 6: Block diagram of the proposed PV system.

The DC-DC converter used is a Buck-Boost converter. It is designed for continuous conduction current mode with the following specifications: $C_1 = 440$ μF, $C_2 = 330$ μF, $L = 0.7$ mH and a chopping frequency of 50 kHz.

The parameters used in the implementation of the BA-MPPT algorithm are as follows: $N = 3$, $\omega = 0.4$, $\alpha = 0.9$, $\gamma = 0.6$, $\Delta d = 0.01$ and $\Delta P = 0.05$. After applying each duty cycle, we should wait for the transient condition to settle. Indeed, the time required for the system to reach the steady state can vary according to the difference between two successive duty cycles. This difference can be more or less important, which affects the dynamics of the

DC-DC converter and its settle time. To determine the appropriate sampling time for the MPPT controller, the tracking response is analysed when the PV system is subjected to uniform irradiance of $G = 1000$ W/m^2. Starting with an initial sample time of 0.1 s, the tracked voltage is examined to determine the optimal sample time which permits to the system to reach the steady state. Fig. 7 presents the tracked PV voltage using the bat algorithm. From this figure, it can be noticed that the settle time of the system is varying. Therefore, an appropriate choice of the sampling time for the MPPT controller is required in order to have correct samples of PV current and PV voltage. If wrong values of PV current and PV voltage are sensed (measured in transient state of the system), the considered PV power values will be wrong. Therefore, the determination of the best duty cycle may be affected, which can influence the accuracy of the tracking of maximum power point. From Fig. 7, it can be noticed that 0.05 s is a reasonable choice.

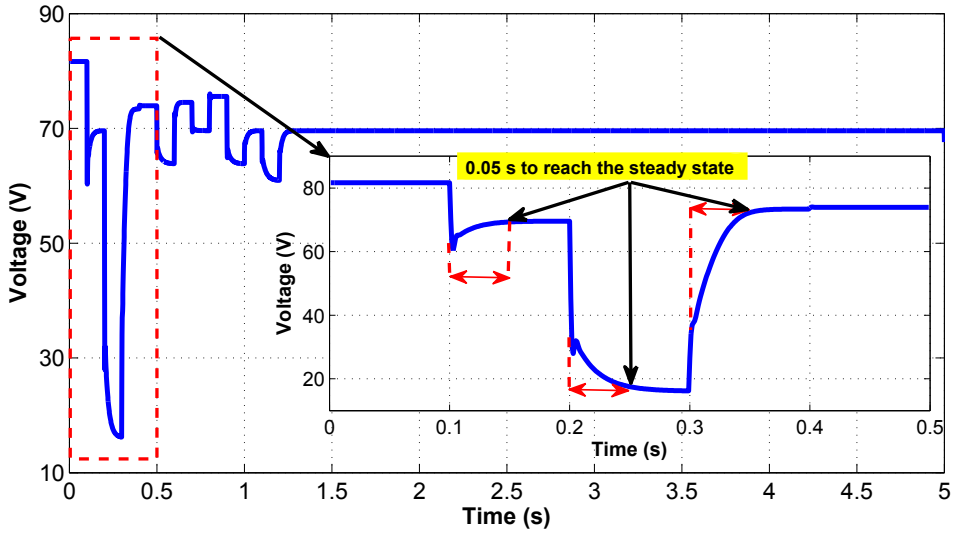

Figure 7: Determination of BA based MPPT sampling time.

Initially, the proposed algorithm is tested for three different configurations of partial shading. Fig. 8 shows the various P-V characteristics corresponding of the configurations as well as the sequence of test. The first P-V curve is characterized by the presence of five (5) maximum power points. The global maximum point is located to the right of this curve. The second configuration presents partial shading with the moving of global maximum power point to the middle of the P-V curve whereas this point moves to the left in the third configuration. Each shading configuration lasts 5 seconds.

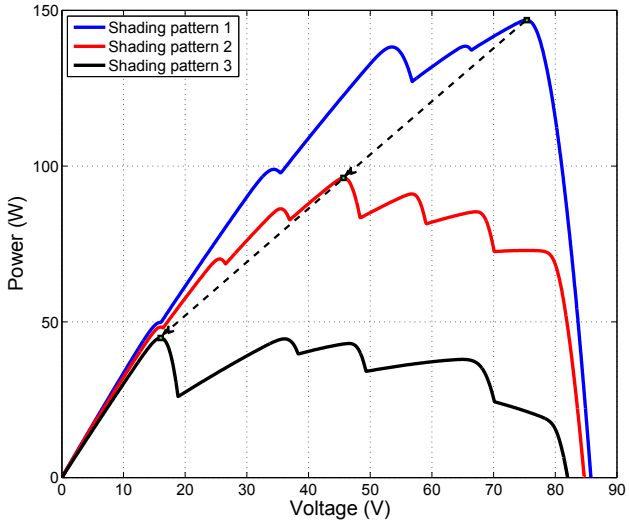

Figure 8: P-V curve used in the simulation.

Fig. 9 shows the results of the dynamic tracking. Initially, the bat algorithm transmitted the first solution vector (the first three duty cycles) and begins the optimization process. It can be seen that the proposed bat algorithm is able to distinguish between the global maximum ($P_{GMPP} = 146.85$ W) and the local maximas. At $t = 5$ s, the configuration of the shading

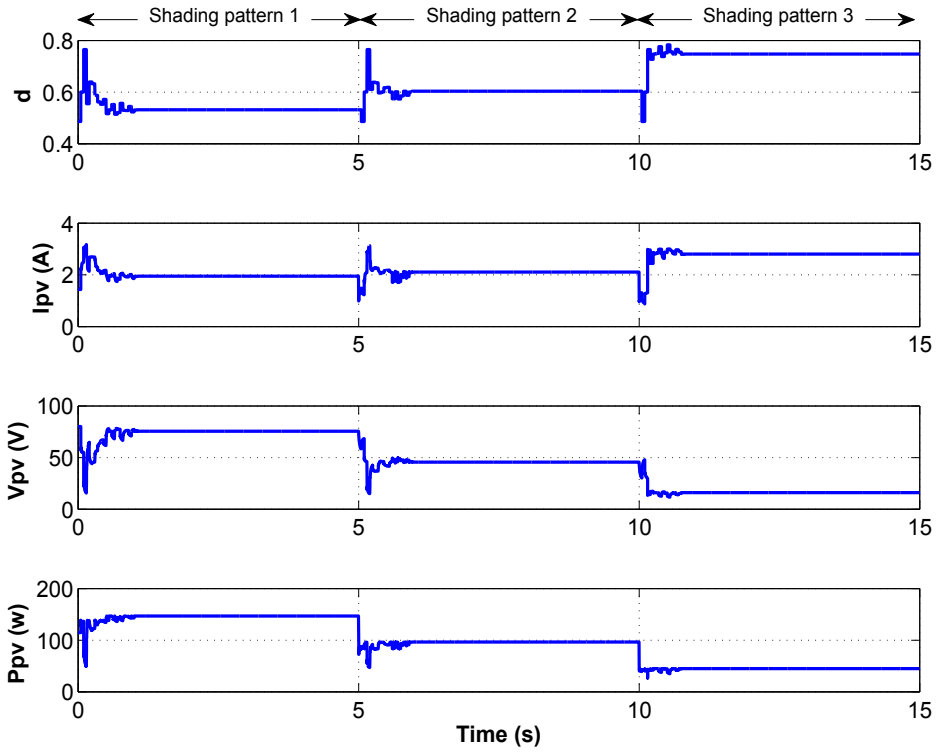

Figure 9: Variation of duty cycle, current, voltage and power of the PV system during GMPP tracking using BA based MPPT.

changes. The proposed algorithm detects this change through information on the power of the photovoltaic panel that changes from $P = 146.85$ W to $P = 86.8$ W. The process of the tracking is then re-initialised and the algorithm has successfully locates the new global maximum which corresponds to $V = 45.63$ V and $I = 2.11$ A. At $t = 10$ s, the global maximum is shifted to the left of the P-V curve. The power of the photovoltaic panel has changed from $P = 96.21$ W to $P = 39.3$ W, and the condition of re-initialisation is then satisfied. The proposed algorithm has re-initialised the searching pro-

cess and the new GMPP is also detected.

As mentioned in the section I, the proposed bat algorithm uses a technique of automatic switching between the exploration stage (global search) and exploitation stage (local search). To illustrate this failover, we can define the function S as follows

$$S = \begin{cases} 1 & if \quad d = d_{global} \\ 0 & if \quad d = d_{local} \end{cases} \tag{20}$$

Fig. 10 shows the variation of the function S as a function of time. The function S is 1 when the duty cycle resulting from the global search is selected. Otherwise, when the duty cycle from the local search that is selected, the function S is 0. For example, consider the first configuration of the shading shown on the zoom of the Fig. 10. A MPPT cycle is achieved after evaluating all the three duty cycles. Therefore, a MPPT cycle corresponds to three perturbations. For the first vector of solutions, it is assumed that this is a global search. This assumption is justified by the fact that the first three duty cycles are selected to "explore" efficiently the search space. Therefore, S is initially 1.

In the second MPPT cycle, it can be noticed that the algorithm has applied an automatic zoom to the region where the best duty cycle is located (the duty cycle which gives the best value of photovoltaic panel power). In this cycle, it is the local search that is selected for the three duty cycles. Automatic switching between the stage of exploration and exploitation appears significantly in the third MPPT cycle. For the first and third duty cycle, it is the local search that is selected while for the second, it is the duty cycle

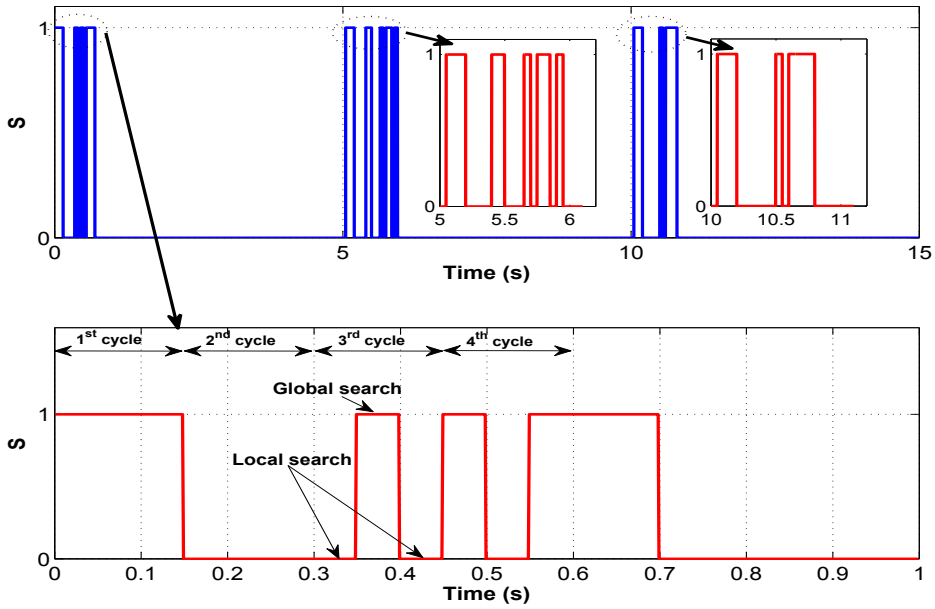

Figure 10: Variation of type of search (global or local) during the MPPT process.

generated from the global search that is chosen. Therefore, the exploration-exploitation tradeoff is very strong. This feature allows the bat algorithm to have a quick convergence rate towards the global maximum without falling into the trap of premature convergence. The advantages of the proposed algorithm appear also in the selection of the algorithm parameters. Many metaheuristics applied to MPPT use either fixed parameters (for standard versions) or adaptive parameters (in enhanced versions). In this second case, the tuning of the parameters is generally done depending on iterations. In contrast, the proposed bat algorithm uses parameter control. Indeed, the values of the algorithm parameters (A and r) are updated not only according to the iterations, but also according to the values of the objective function

and loudness. This strategy provides a mechanism of automatic switching from exploration to exploitation when the global maximum is approached.

The performances of the proposed algorithm are compared with two algorithms, PSO and P&O. The parameters used for PSO algorithm are $w = 0.4$, $c_1 = 0.5$ and $c_2 = 0.75$. These parameters are selected after a series of simulations on the shading configurations under test; therefore, it can be confirmed that the selected combination (w, c_1, c_2) is optimal. The first population, the convergence criterion and that of re-initialisation are the same as for the proposed bat algorithm. For P&O algorithm, a fixed perturbation step of $\Delta d_{P\&O} = 0.01$ is imposed every 0.05 s. Fig. 11 and Fig. 12 show the results of the tracking for the PSO algorithms and P&O, respectively.

As can be seen, the PSO algorithm has detected the changes in the shading configurations and the re-initialisation of the MPPT process. It also successfully locates the global maxima in the three configurations. In contrast, compared with the results obtained by the proposed algorithm, it can be observed that the bat algorithm gives the best results in static and presents the best dynamic behavior. This is supported by the results of the calculation of the static and dynamic efficiency. The static efficiency is given by

$$\eta_{static} = \frac{P_{MPPT}}{P_{max}} \tag{21}$$

where P_{MPPT} is the power obtained in the steady state condition and P_{max} is the maximum power available on the photovoltaic panel.

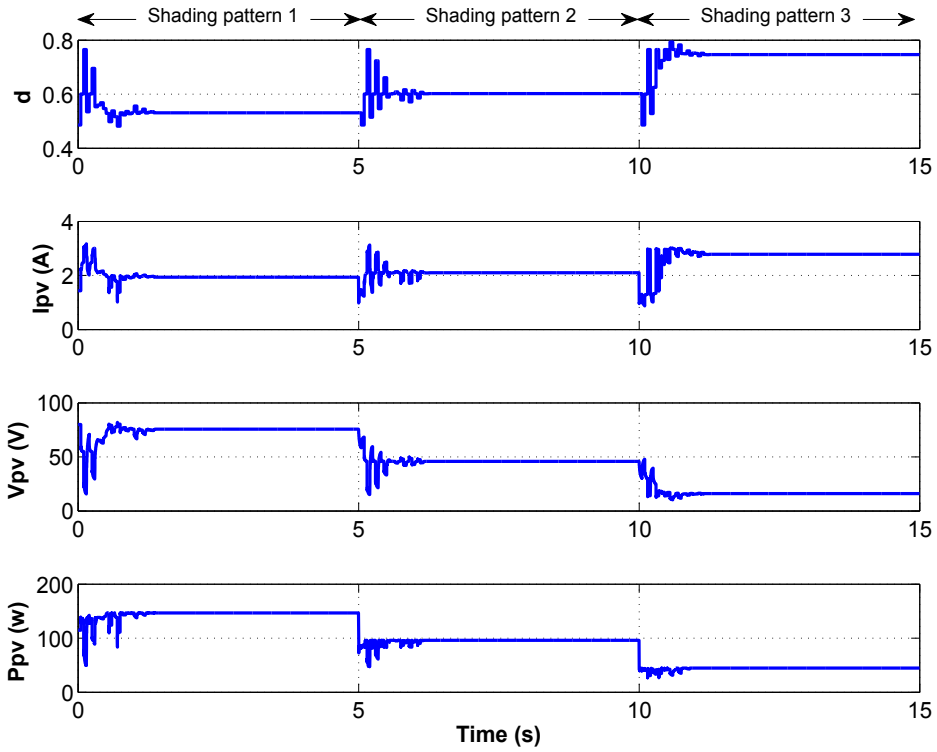

Figure 11: Variation of duty cycle, current, voltage and power of the PV system during GMPP tracking using PSO based MPPT.

The dynamic performance takes into account the transient time and the steady state condition. It is calculated as

$$\eta_{dynamic} = \frac{\int_0^T P_{PV} dt}{\int_0^T P_{max} dt} 100 = \frac{\int_0^{15} P_{PV} dt}{\int_0^{15} P_{max} dt} 100. \tag{22}$$

Table 2 shows the results of the tracking in steady state condition. The results of the calculation of the dynamic efficiency of BA and PSO are 98.36 and 97.87, respectively. Although the PSO algorithm presents good static efficiency, the fluctuations in the voltage are very high compared to the pro-

Table 2: Comparaison between the proposed BA-MPPT method PSO-MPPT method in steady state condition.

Curve no.	Ideal power P_{max} (W)	Power obtained P_{MPPT} (W)		Static efficiency (η_{static})	
		BA	PSO	BA	PSO
Curve 1	146.87	146.85	146.72	99.98	99.90
Curve 2	96.22	96.21	96.19	99.98	99.97
Curve 3	44.83	44.82	44.82	99.97	99.97

posed method. In addition, the advantage of the proposed method appears in its faster convergence speed. For the first shading pattern, the PSO algorithm takes 9 MPPT cycles (27 perturbations) to meet the convergence criterion whereas the proposed method takes only 7 cycles. It can be noticed that the proposed method locates the region of the GMPP in less than 5 MPPT cycles and activates only the local search after 15 perturbations. For the second shading configuration, the bat algorithm performs 18 perturbations to reach the steady state, less than the PSO algorithm by 4 perturbations. Furthermore, for the third shading pattern, the PSO algorithm lasts 8 MPPT cycles and the bat algorithm requires only 5 MPPT cycles to settle at the GMPP.

These results are justified by the fact that the bat algorithm combines the global search and local search in the optimization process. This combination avoids large fluctuations and disturbances in the photovoltaic panel voltage and provides better control of the search space.

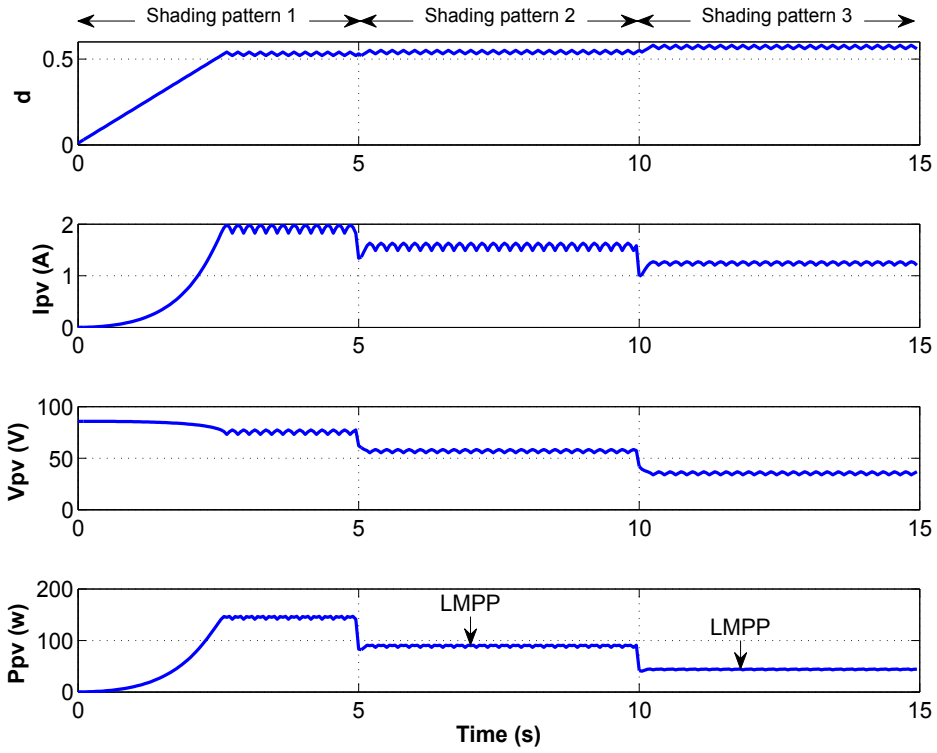

Figure 12: Variation of duty cycle, current, voltage and power of the PV system during GMPP tracking using P&O algorithm.

Fig. 12 also shows the results obtained by the P&O algorithm. For the first configuration, the P&O algorithm has successfully located the GMPP, which is found to the right of the P-V characteristic. For the other configurations, the algorithm could not distinguish the GMPP from LMPPs and trapped in an LMPP. These results prove the inability of the P&O algorithm to handle the case of partial shading.

Table 3: Steady state tracking results for the proposed BA based MPPT and PSO technique under various shading patterns.

	Shading pattern (1 = 1000 W/m^2)								Global peak values			Proposed BAT-MPPT			PSO-MPPT			Static efficiency	
	G_{11}	G_{12}	G_{21}	G_{22}	G_{31}	G_{32}	G_{41}	G_{42}	V_{GMPP} (V)	I_{GMPP} (A)	P_{GMPP} (P)	V_{MPPT} (V)	I_{MPPT} (A)	P_{MPPT} (P)	V_{MPPT} (V)	I_{MPPT} (A)	P_{MPPT} (P)	BA	PSO
1	1	1	1	1	1	1	1	1	69.78	3.15	219.25	69.6	3.15	219.24	69.6	3.15	219.24	99.99	99.99
2	1	1	0.9	0.9	0.8	0.8	0.6	0.6	74.88	1.94	144.64	75.04	1.93	144.62	74.12	1.95	144.33	99.98	99.79
3	1	1	0.9	0.9	0.3	0.3	0.2	0.2	34.37	2.88	98.96	34.94	2.82	98.65	35.23	2.79	98.2	99.68	99.23
4	1	1	0.8	0.8	0.7	0.7	0.4	0.4	54.08	2.26	121.77	53.88	2.26	121.74	54.91	2.21	121.21	99.97	99.54
5	1	1	0.9	0.9	0.8	0.8	0.7	0.5	64.56	2.29	147.49	64.57	2.28	147.48	64.14	2.3	147.33	99.99	99.89
6	0.7	0.7	0.6	0.6	0.45	0.45	0.3	0.1	54.74	1.42	77.44	55.05	1.41	77.39	55.61	1.38	77	99.93	99.43
7	1	1	0.5	0.5	0.2	0.2	0.3	0.1	36.04	1.57	56.48	36.18	1.56	56.47	35.21	1.59	56.11	99.98	99.34
8	1	1	0.9	0.9	0.8	0.7	0.6	0.5	65.86	1.95	128.26	66	1.94	128.24	66.51	1.92	127.76	99.98	99.61
9	1	1	0.6	0.6	0.5	0.4	0.3	0.1	46.17	1.6	73.77	46.32	1.59	73.74	45.27	1.62	73.31	99.96	99.38
10	1	0.9	0.8	0.7	0.6	0.5	0.4	0.3	56.34	1.61	90.37	56.56	1.6	90.33	56.92	1.58	90.01	99.95	99.6

Table 3 summarizes the tracking results of the proposed bat algorithm and the PSO technique for 10 different configurations of shading. The P-V characteristics corresponding to these configurations provide an example of the influence of partial shading on the output power of the photovoltaic panel. These P-V curves can have different number of MPP and the location of the GMPP is variable, making its tracking difficult. As shown in Table 3, the proposed method has accurately located the GMPP for all P-V characteristics studied. It can be seen that it has a static efficiency above 99.9 % for the most of cases. This results from the fact that the proposed bat algorithm uses a combination of global search and intensive local search. The small step size of the perturbation in the local search allows the algorithm to exploit more effectively the best solution. As a result, the bat algorithm has high accuracy in the search of the optimal solution.

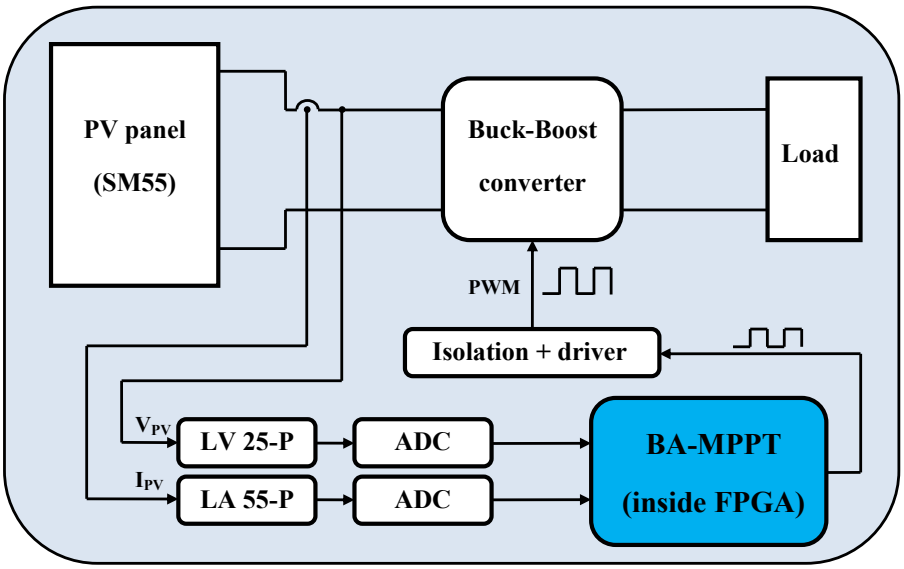

Figure 13: Schematic of connections in the experimental PV system with the proposed MPPT controller.

5. Experimental verification

Fig. 13 shows the experimental system developed for the validation of the proposed bat algorithm. The power converter used is a buck-boost converter designed to operate in continuous conduction current mode. The specifications of the converter are shown in Table 4.

The acquisition circuit of current and voltage of the photovoltaic panel is based on sensors LA 55-P and LV 25-P, respectively. Two ADCs, ADC0804 are used to convert the obtained analog images of current and voltage into digital values for the MPPT controller.

Table 4: Specifications of the Buck-Boost converter.

Parameters	Value
Capacitor C1	440 μF
Capacitor C2	330 μF
Inductance	0.7 mH
Switch	MOSFET IRFP450 (500 V,14 A)
Diode	MUR1640 (400 V,16 A)
Switching frequency	50 kHz

The proposed bat algorithm is implemented on an FPGA circuit XC5VLX50-1FFG676 of Vertex5 family [35]. This circuit is built around an ML501 development board. The codes are written in VHDL and are synthesized with ISE 10.1 of Xilinx.

FPGAs are Very large Scale Integration (VLSI) components. They are programmable by the designer and mainly constituted by three parts:
A matrix of configurable logic blocks (CLB).
Configurable input/output blocs (IOB).
Programmable resources for interconnection.

The use of FPGA circuit for the implementation of MPPT control algorithms offers many advantages. Indeed, FPGA offers real hardware implementation of MPPT algorithm. Taking advantage of hardware parallelism, FPGAs overtake the computing performance of digital signal processors (DSPs) and perform more operations per clock cycle. Therefore, these

circuits offer the possibility of implementing complex control algorithms with low latency of computing time. Also, the speed of FPGAs allows better temporal resolution and improves the performance of MPPT control algorithms.

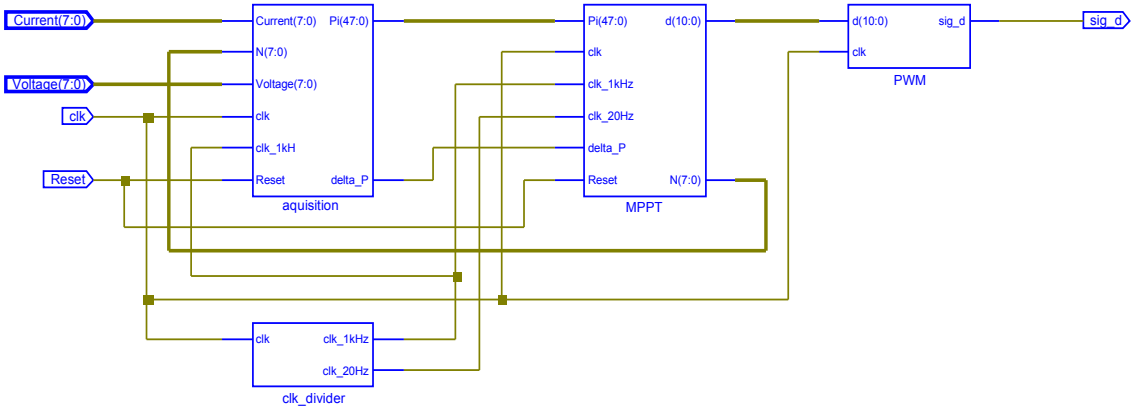

Figure 14: The RTL schematic of the synthesized BA based MPPT.

The Register Transfer Level (RTL) schematic of the synthesized bat algorithm implemented on FPGA is shown in Fig. 14. It includes various blocks coded separately. This modular programming allows a better optimization of hardware resource and a more flexible and reusable structure. The "acquisition" block allows the reading of digital values of the current and voltage generated by the analog-digital converters and the calculating of the value of the photovoltaic panel power. The "clk_divider" block allows the generation, from the clock of the FPGA, of various clocks needed for the functioning and synchronization of different blocks. The "MPPT" block is the key element of calculating of bat algorithm. It comprises several sub-blocks which allow the execution of the deferent instructions of the bat algorithm and the calculation of the duty cycle. The "PWM" block allows the generation of the

Figure 15: Photograph of the experimental setup.

PWM signal from the duty cycle d for the control of the DC-DC converter.

The performance of the proposed algorithm is tested experimentally for four different configurations of partial shading. The photograph of the experimental setup is shown in Fig. 15. The photovoltaic panel is composed of photovoltaic modules (SM55) connected in series. The PV panel is exposed to real irradiance conditions. Since it is difficult to predict exactly the appearance moment of partial shading, this latter is created artificially by blocking small portions of the PV panel. This is done by using sheets of different dimensions.

Fig. 16-19 show the recorded experimental results for the four tests. Each one of these figures includes the P-V characteristic in the presence of partial shading, the voltage, the current and power of the photovoltaic panel during the tracking process. Fig. 16 shows the experimental results obtained for the first test. The first configuration is characterized by the presence of

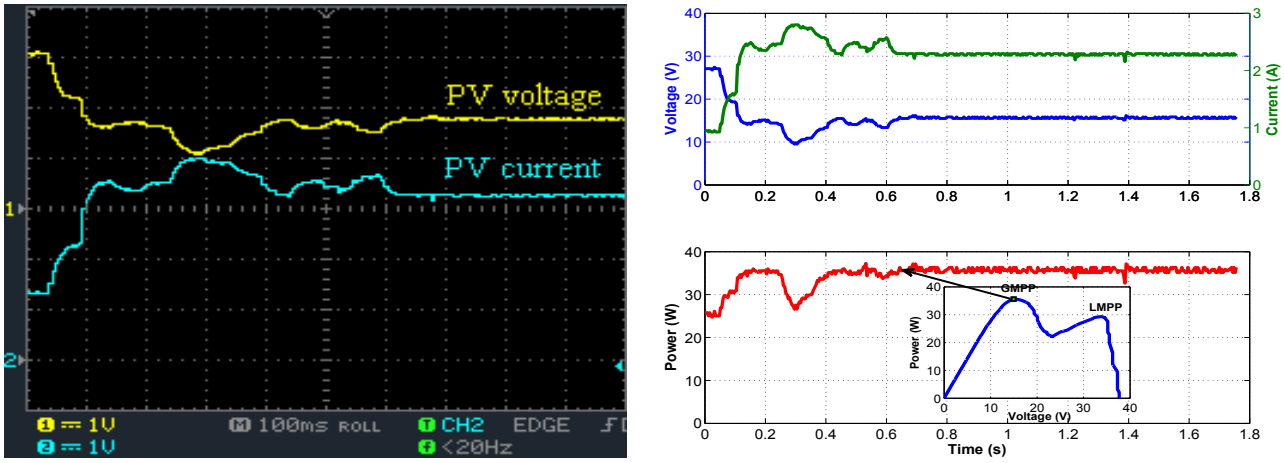

(a) (b)

Figure 16: Measured array current, voltage and power waveforms under shading pattern 1 during MPPT process.

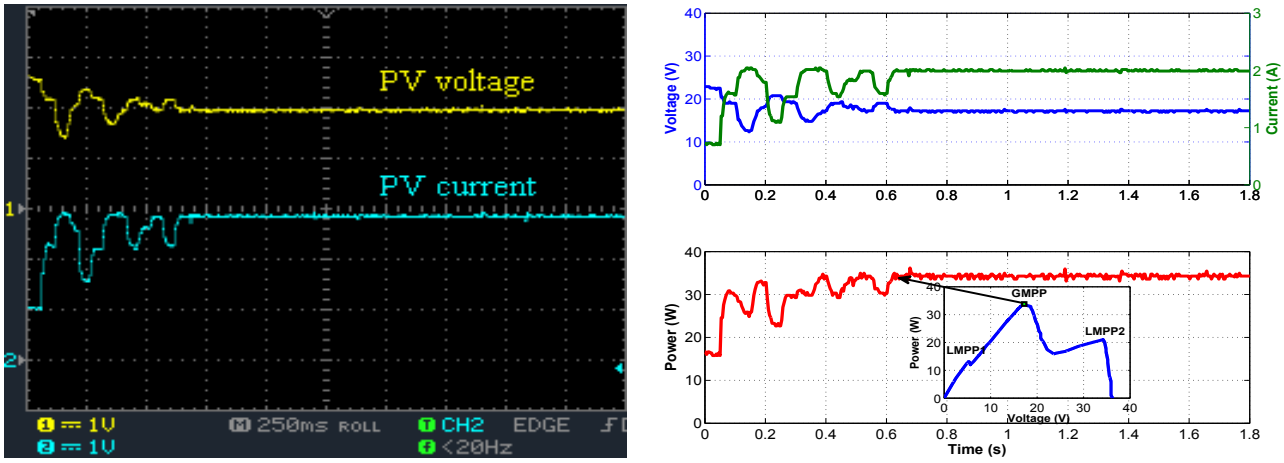

(a) (b)

Figure 17: Measured array current, voltage and power waveforms under shading pattern 2 during MPPT process.

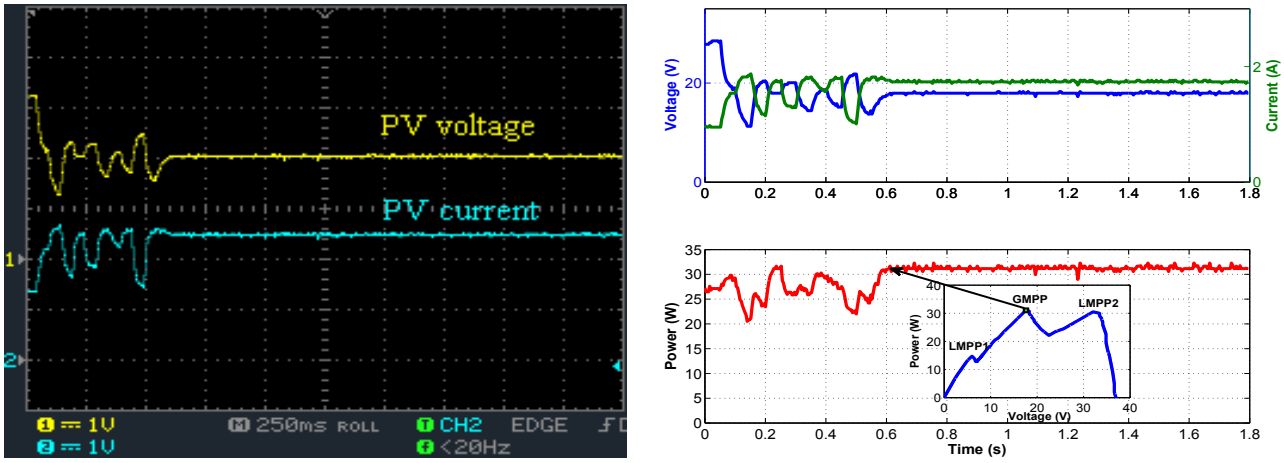

(a) (b)

Figure 18: Measured array current, voltage and power waveforms under shading pattern 3 during MPPT process.

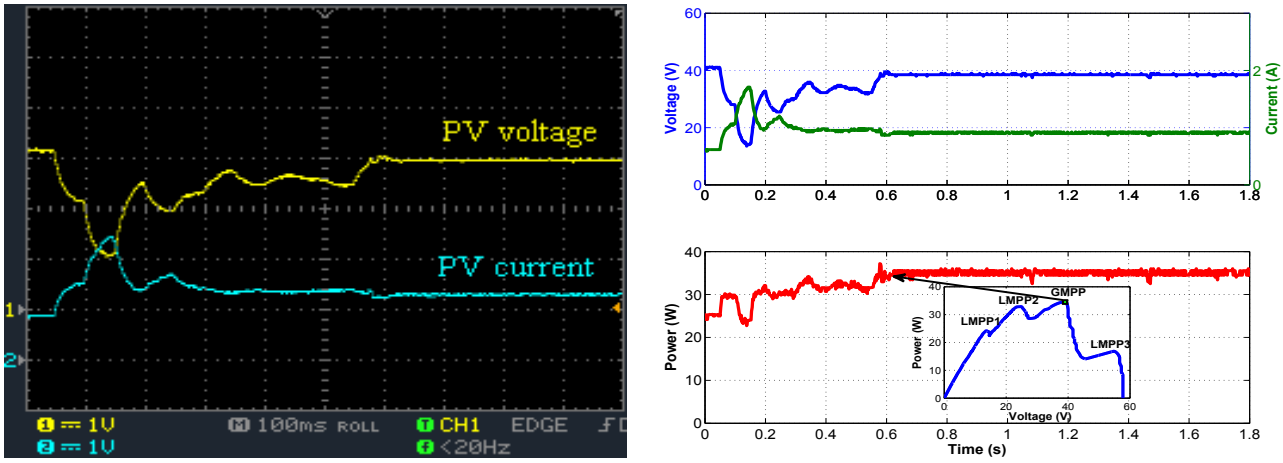

(a) (b)

Figure 19: Measured array current, voltage and power waveforms under shading pattern 4 during MPPT process.

two points of maximum power, $P_{LMPP} = 29.33$ W and $P_{GMPP} = 35.6$ W, respectively. The global maximum power point is to the left of the P-V curve, at $V_{GMPP} = 15$ V. It can be noticed that the bat algorithm has successfully located the GMPP and the operating point is maintained around $V = 15.49$ V and $I = 2.29$ A.

In the second and the third cases shown in Fig. 17 and Fig. 18, the P-V characteristic has three points of maximum power. In the second case, the global maximum power point, $P_{GMPP} = 33.81$ W is in the middle of the P-V curve at $V_{GMPP} = 17.25$ V. The proposed algorithm was able to distinguish the GMPP from the LMPPs and the steady state is reached after four MPPT cycles. In the third case, the global maximum point (GMPP) and the local maximum point (LMPP2) are at very close power levels, $P_{GMPP} = 31.05$ W and $P_{LMPP2} = 30.46$ W, respectively. The bat algorithm effectively tracked the GMPP and the voltage of the photovoltaic panel is maintained around $V = 17.95$ V.

The effectiveness of the proposed scheme is proved also when the PV array is subjected to extreme partial shading condition. In the fourth shading pattern shown in Fig. 19, the P-V characteristic curve exhibits four (4) peaks. For this configuration, the proposed MPPT controller implemented into FPGA has also successfully tracked the GMPP at $V = 38.48$ V and $I = 0.92$ A.

6. Conclusion

In this paper, a MPPT algorithm based on a bat algorithm is proposed to deal with the multi-modal characteristic of photovoltaic panel under par-

tial shading conditions. The key features of the BA are explained in details. This algorithm can provide very quick convergence and high accuracy since it dynamically combines the explorations moves with the extensive local search during the MPPT process. Simulations are carried out under extreme shading patterns to confirm the global search ability and the good dynamic performance. The simulations results show that the proposed method tracks the GMPP with a high accuracy and yields a static efficiency above 99.9 % for the most cases studied. In addition, the proposed scheme outperforms the P&O and the PSO methods in terms of accuracy and oscillations in PV power at the transient time. FPGA implementation is presented to validate the proposed algorithm on real time application. Being reconfigurable, FPGAs can offer a high degree of flexibility and robustness. Since the PWM signal is generated with a high resolution, the performance of the tracking process is largely improved. Experimental results confirm the efficiency of the proposed method in the global peak tracking and the accuracy under partial shading conditions.

[1] A. Mellit, S. Kalogirou, L. Hontoria, S. Shaari, Artificial intelligence techniques for sizing photovoltaic systems: A review, Renewable and Sustainable Energy Reviews 13 (2) (2009) 406–419.

[2] F. Belhachat, C. Larbes, Modeling, analysis and comparison of solar photovoltaic array configurations under partial shading conditions, Solar Energy 120 (2015) 399–418.

[3] A. Woyte, J. Nijs, R. Belmans, Partial shadowing of photovoltaic arrays with different system configurations: literature review and field test results, Solar Energy 74 (3) (2003) 217–233.

[4] E. Karatepe, M. Boztepe, M. Colak, Development of a suitable model for characterizing photovoltaic arrays with shaded solar cells, Solar Energy 81 (8) (2007) 977–992.

[5] P. Bhatnagar, R. Nema, Maximum power point tracking control techniques: State-of-the-art in photovoltaic applications, Renewable and Sustainable Energy Reviews 23 (2013) 224–241.

[6] A. Dolara, G. C. Lazaroiu, S. Leva, G. Manzolini, Experimental investigation of partial shading scenarios on pv (photovoltaic) modules, Energy 55 (2013) 466–475.

[7] R. Eke, C. Demircan, Shading effect on the energy rating of two identical pv systems on a building façade, Solar Energy 122 (2015) 48–57.

[8] A. Bidram, A. Davoudi, R. S. Balog, Control and circuit techniques to mitigate partial shading effects in photovoltaic arrays, IEEE Journal of Photovoltaics 2 (4) (2012) 532–546.

[9] A. Kouchaki, H. Iman-Eini, B. Asaei, A new maximum power point tracking strategy for pv arrays under uniform and non-uniform insolation conditions, Solar Energy 91 (2013) 221–232.

[10] J. Ahmed, Z. Salam, A critical evaluation on maximum power point tracking methods for partial shading in pv systems, Renewable and Sustainable Energy Reviews 47 (2015) 933–953.

[11] Y.-H. Liu, J.-H. Chen, J.-W. Huang, Global maximum power point tracking algorithm for pv systems operating under partially shaded conditions using the segmentation search method, Solar Energy 103 (2014) 350–363.

[12] T. L. Nguyen, K.-S. Low, A global maximum power point tracking scheme employing direct search algorithm for photovoltaic systems, IEEE transactions on Industrial Electronics 57 (10) (2010) 3456–3467.

[13] K. Lian, J. Jhang, I. Tian, A maximum power point tracking method based on perturb-and-observe combined with particle swarm optimization, IEEE journal of photovoltaics 4 (2) (2014) 626–633.

[14] R.-Y. Kim, J.-H. Kim, An improved global maximum power point tracking scheme under partial shading conditions, in: Journal of International Conference on Electrical Machines and Systems, Vol. 2, Journal of International Conference on Electrical Machines and Systems, 2013, pp. 65–68.

[15] B. N. Alajmi, K. H. Ahmed, S. J. Finney, B. W. Williams, A maximum power point tracking technique for partially shaded photovoltaic systems

in microgrids, IEEE Transactions on Industrial Electronics 60 (4) (2013) 1596–1606.

[16] R. Boukenoui, H. Salhi, R. Bradai, A. Mellit, A new intelligent mppt method for stand-alone photovoltaic systems operating under fast transient variations of shading patterns, Solar Energy 124 (2016) 124–142.

[17] M. Miyatake, M. Veerachary, F. Toriumi, N. Fujii, H. Ko, Maximum power point tracking of multiple photovoltaic arrays: a pso approach, IEEE Transactions on Aerospace and Electronic Systems 47 (1) (2011) 367–380.

[18] K. Ishaque, Z. Salam, A. Shamsudin, M. Amjad, A direct control based maximum power point tracking method for photovoltaic system under partial shading conditions using particle swarm optimization algorithm, Applied Energy 99 (2012) 414–422.

[19] K. Ishaque, Z. Salam, A deterministic particle swarm optimization maximum power point tracker for photovoltaic system under partial shading condition, IEEE transactions on industrial electronics 60 (8) (2013) 3195–3206.

[20] Y.-H. Liu, S.-C. Huang, J.-W. Huang, W.-C. Liang, A particle swarm optimization-based maximum power point tracking algorithm for pv systems operating under partially shaded conditions, IEEE Transactions on Energy Conversion 27 (4) (2012) 1027–1035.

[21] K.-H. Chao, Y.-S. Lin, U.-D. Lai, Improved particle swarm optimiza-

tion for maximum power point tracking in photovoltaic module arrays, Applied Energy 158 (2015) 609–618.

[22] M. F. N. Tajuddin, S. M. Ayob, Z. Salam, M. S. Saad, Evolutionary based maximum power point tracking technique using differential evolution algorithm, Energy and Buildings 67 (2013) 245–252.

[23] K. S. Tey, S. Mekhilef, H.-T. Yang, M.-K. Chuang, A differential evolution based mppt method for photovoltaic modules under partial shading conditions, International Journal of Photoenergy 2014.

[24] M. A. Ramli, K. Ishaque, F. Jawaid, Y. A. Al-Turki, Z. Salam, A modified differential evolution based maximum power point tracker for photovoltaic system under partial shading condition, Energy and Buildings 103 (2015) 175–184.

[25] J. Ahmed, Z. Salam, A maximum power point tracking (mppt) for pv system using cuckoo search with partial shading capability, Applied Energy 119 (2014) 118–130.

[26] K. Sundareswaran, S. Peddapati, S. Palani, Mppt of pv systems under partial shaded conditions through a colony of flashing fireflies, IEEE Transactions on Energy Conversion 29 (2) (2014) 463–472.

[27] M. Seyedmahmoudian, R. Rahmani, S. Mekhilef, A. M. T. Oo, A. Stojcevski, T. K. Soon, A. S. Ghandhari, Simulation and hardware implementation of new maximum power point tracking technique for partially shaded pv system using hybrid depso method, IEEE Transactions on Sustainable Energy 6 (3) (2015) 850–862.

[28] M. Seyedmahmoudian, B. Horan, T. K. Soon, R. Rahmani, A. M. T. Oo, S. Mekhilef, A. Stojcevski, State of the art artificial intelligence-based mppt techniques for mitigating partial shading effects on pv systems–a review, Renewable and Sustainable Energy Reviews 64 (2016) 435–455.

[29] X.-S. Yang, A new metaheuristic bat-inspired algorithm, in: Nature inspired cooperative strategies for optimization (NICSO 2010), Springer, 2010, pp. 65–74.

[30] K. Ishaque, Z. Salam, et al., A comprehensive matlab simulink pv system simulator with partial shading capability based on two-diode model, Solar Energy 85 (9) (2011) 2217–2227.

[31] X.-S. Yang, M. Karamanoglu, S. Fong, Bat algorithm for topology optimization in microelectronic applications, in: The First International Conference on Future Generation Communication Technologies, IEEE, 2012, pp. 150–155.

[32] X.-S. Yang, Bat algorithm and cuckoo search: a tutorial, in: Artificial Intelligence, Evolutionary Computing and Metaheuristics, Springer, 2013, pp. 421–434.

[33] S. Yilmaz, E. U. Kucuksille, Improved bat algorithm (iba) on continuous optimization problems, Lecture Notes on Software Engineering 1 (3) (2013) 279.

[34] V. Quaschning, R. Hanitsch, Numerical simulation of current-voltage characteristics of photovoltaic systems with shaded solar cells, Solar Energy 56 (6) (1996) 513–520.

[35] http://www.xilinx.com.